Analytical method for the ultrasonic characterization of homogeneous rigid porous materials from transmitted and reflected coefficients

J.-P. Groby[a)]
Département de Recherche en Électromagnétisme-Laboratoire de Signaux et Systèmes, UMR8506 CNRS/Supélec/Univ. Paris-Sud, F-91192 Gif-sur-Yvette, France

E. Ogam
Laboratoire de Mécanique et d'Acoustique, UPR7051 CNRS, F-13402 Marseille Cedex 20, France

L. De Ryck,[b)] N. Sebaa, and W. Lauriks
Laboratory of Acoustics and Thermal Physics, K.U.Leuven, B-3001 Heverlee, Belgium

(Received 8 December 2008; revised 9 December 2009; accepted 11 December 2009)

A frequency domain method dedicated to the analytic recovery of the four relevant parameters of macroscopically homogeneous rigid frame porous materials, e.g., plastic foams, at the high frequency range of the Johnson–Champoux–Allard model is developed and presented. The reconstructions appeal to experimental data concerning time domain measurements of the ultrasonic fields reflected and transmitted by a plate of the material at normal incidence. The effective density and bulk modulus of the material are first reconstructed from the frequency domain reflection and transmission coefficients. From the latter, the porosity, tortuosity, and thermal and viscous characteristic lengths are recovered. In a sense, the method presented herein is quite similar in the ultrasonic range, but also quite complementary, to the method developed by Panneton and Olny [J. Acoust. Soc. Am. **119**, 2027–2040 (2006); **123**, 814–824 (2008)] at low frequency, which appeal to experimental data measured in an impedance tube.
 [DOI: 10.1121/1.3283043]

PACS number(s): 43.35.Zc, 43.20.Jr, 43.20.Ye, 43.40.Sk [KVH] Pages: 764–772

I. INTRODUCTION

A rigid frame porous material is a porous material whose frame is immobile. This assumption is not only conditioned by the saturating fluid usually a light fluid such as air, but also by the frequency of the acoustic solicitation. The frequency band suitable for the rigid frame approximation is bounded at high frequency by the diffusion limit, when the wavelength is of the order of, or smaller than the pore size, and at low frequency by the fluid-solid decoupling frequency below which the skeleton may vibrate. These bounds depend on the material properties, and so on its characteristics.

The equations of motion in a rigid frame porous material, derived from Biot's theory[1,2] and in later publications,[3–8] reduce to those of an equivalent fluid, with complex frequency-dependent effective density and bulk modulus. These later publications present semiphenomenological models that describe the viscous and thermal dissipations over specific frequency ranges, assuming known the characteristics of the saturating fluid, i.e., the viscosity η, the saturating pressure P_0, the specific heat ratio γ, and density ρ_f. Concerning the viscous dissipation, the Johnson *et al.* model[3] was made to fit the exact high- and low- (imaginary) frequency limits of the effective density, while the Wilson[7] model was contrived to match the mid frequency range of the latter. Concerning the thermal dissipation, the Champoux–Allard model[4] was developed to fit the exact high frequency limits of the effective bulk modulus, while the Wilson[7] model was contrived to match the mid frequency range of the latter. Inspired by the fact that the low frequency development of the Champoux–Allard model is not exact, Lafarge *et al.*[6] proposed an alternative expression of the effective bulk modulus and introduce the static thermal permeability. However, this parameter seems to be difficult to determine, even at low frequency.[6,9,10]

Herein, the Johnson–Champoux–Allard model[3,4] (JCAM) is considered, because high frequency measurements are performed. The parameters involved in this model are the porosity ϕ, which is the ratio of the fluid volume to the total sample volume; the tortuosity α_∞, which describes the change in magnitude and direction of the fluid microvelocity due to curliness of the pores; the characteristic viscous and thermal lengths Λ and Λ', which relate to the geometry of the pores through the viscous and thermal losses; and the flow resistivity σ, which is the ratio of the fluid viscosity η to the fluid permeability κ_f. The inverse problem consists in recovering some or all of these five parameters from measurements of the scattered fields, i.e., the reflected and transmitted fields in the case of a rigid frame porous plate.

Subsequent to the experimental apparatus of Beranek[11] to determine the porosity (porosimeter), or the flowmeter of Brown and Bolt[12] to determine the flow resistivity, several methods have been developed to characterize macroscopi-

[a)]Author to whom correspondence should be addressed. Electronic mail: jean-philippe.groby@univ-lemans.fr. Present address: Laboratoire d'Acoustique de l'Université du Maine, UMR6613 CNRS/Univ. du Maine, F-72085 Le Mans Cedex 9, France.
[b)]Present address: LMS international NV, B-3001 Leuven, Belgium.

cally homogeneous porous samples, or layered porous samples. From ultrasonic measurements, methods developed either in the frequency or in the time domain allow the determination of the porosity,[13] the tortuosity,[14] the porosity and tortuosity simultaneously,[15] the viscous and thermal characteristic lengths[16] (using the $Q\delta$ method), or the porosity, tortuosity, and viscous characteristic length (the thermal characteristic length being set to three times the viscous one) simultaneously.[17,18] Specific methods have been developed for the characterization of highly absorbent porous materials, based on the variation of the static pressure of the saturating fluid,[19] mainly for the determination of the viscous characteristic length and the tortuosity. Recently, the simultaneous reconstruction of the three profiles of porosity, tortuosity, and viscous characteristic length of a macroscopically inhomogeneous rigid frame porous plate from simulated reflection coefficients for various angles of incidence was carried out[20] through an optimization process.

A characteristic of these many studies and methods, particularly in the frequency domain, is the difference in sensitivity of each parameter on the physical quantities. For example, both the density and bulk modulus do not depend on σ in the asymptotic high frequency range. Moreover, most of the methods for the simultaneous reconstruction of the parameters appeal to minimization techniques.[18,19] On the other hand, two analytic methods were developed[9,10] appealing to measurements in an impedance tube.[21] The idea is first to reconstruct the equivalent density and bulk modulus for various frequencies from the measurement of the impedance and the acoustic index of refraction and then to recover the parameters involved in several dissipation models mainly through analytic inversion, but also after extrapolation if needed. This leads to four equations at each frequency formed by the real and imaginary parts of the effective density and bulk modulus. Concerning the JCAM, these methods enable the recovery of the tortuosity, viscous and thermal characteristic lengths, and flow resistivity assuming the porosity to be known. This assumption seems to be due to the necessary use of the complex form of the complete JCAM, which involves five parameters, for the correct modeling of the phenomena in the frequency range considered therein. For the number of to-be-reconstructed parameters to be lower than or equal to the number of equations, a simplified model should be used, for example, the asymptotic high frequency one. In this ultrasonic frequency range, only four parameters are relevant. Complete analytical recovery of the latter is also enabled from the knowledge of the *complex* density and bulk modulus. The low frequency bound of this asymptotic regime is not clear and depends on the material, but it can be assumed that for frequencies higher than 100 kHz, this regime is reached for most of the porous foams. The high frequency bound is the diffusion limit, which is related to some of the parameters to be reconstructed, particularly the characteristic length.[22]

The aim of this article is to present a simple, efficient, and analytic frequency domain method for the simultaneous recovery of the four parameters appealing to the high frequency approximation of the JCAM, i.e., ϕ, α_∞, Λ, and Λ', for a macroscopically homogeneous rigid frame porous plate saturated by air, i.e., $\eta=1.839\times10^{-5}$ m^2 s^{-1}, $P_0=1.013\,25\times10^5$ Pa, $\rho_f=1.213$ kg m^{-3}, and $\gamma=1.4$, by means of ultrasonic measurements at normal incidence. This method can be considered as complementary to those proposed in Refs. 9 and 10 for a complete analytical characterization of macroscopically homogeneous porous materials.

II. ANALYTICAL CHARACTERIZATION OF A MACROSCOPICALLY HOMOGENEOUS RIGID FRAME POROUS PLATE

In what follows, the pressure $p(x,t)$ is related to its Fourier transform $P(x,\omega)$ through

$$p(x,t)=\int_{-\infty}^{\infty}P(x,\omega)e^{-i\omega t}d\omega. \tag{1}$$

A. Basic theoretical retrieval equations

When solicited by a normally incident plane wave, the reflection $\mathcal{R}(\omega)$ and transmission $\mathcal{T}(\omega)$ coefficients of a homogeneous plate of thickness L occupied by the equivalent fluid medium $M^{[1]}$ and surrounded by the same fluid, denoted as medium $M^{[0]}$, take the following forms:[23]

$$\mathcal{R}=\frac{R(1-e^{2ik^{[1]}L})}{1-R^2e^{2ik^{[1]}L}},$$

$$\mathcal{T}=\frac{(1-R^2)e^{i(k^{[1]}-k^{[0]})L}}{1-R^2e^{2ik^{[1]}L}}, \tag{2}$$

wherein $R=(Z^{[1]}-Z^{[0]})/(Z^{[1]}+Z^{[0]})$ is the reflection coefficient at the interface between two semi-infinite media $M^{[1]}$ and $M^{[0]}$, with $Z^{[j]}=\rho^{[j]}c^{[j]}=\sqrt{K^{[j]}\rho^{[j]}}$ the impedance of $M^{[j]}$, and $\rho^{[j]}$, $c^{[j]}$, and $K^{[j]}$ being the density, sound speed, and bulk modulus, respectively, $j=0,1$. Let us now introduce $S_{11}(\omega)$ and $S_{21}(\omega)$, the coefficients of the scattering matrix $\mathbf{S}$, related to $\mathcal{R}$ and $\mathcal{T}$ through

$$S_{11}=\mathcal{R}=\frac{R(1-e^{2ik^{[0]}\zeta L})}{1-R^2e^{2ik^{[0]}\zeta L}},$$

$$S_{21}=\mathcal{T}e^{ik^{[0]}L}=\frac{(1-R^2)e^{ik^{[0]}\zeta L}}{1-R^2e^{2ik^{[0]}\zeta L}}, \tag{3}$$

wherein $\zeta(\omega)=k^{[1]}/k^{[0]}=c^{[0]}/c^{[1]}=\sqrt{K^{[0]}\rho^{[1]}/K^{[1]}\rho^{[0]}}$ is the acoustic index of refraction, i.e., the ratio between the wavenumbers of media $M^{[1]}$ and $M^{[0]}$. The acoustic index of refraction and the impedance ratio $z(\omega)=Z^{[1]}/Z^{[0]}=\sqrt{K^{[1]}\rho^{[1]}/K^{[0]}\rho^{[0]}}$ can be obtained analytically by inverting Eq. (3), yielding[24–26]

$$z=\pm\sqrt{\frac{(1+S_{11})^2-S_{21}^2}{(1-S_{11})^2-S_{21}^2}}, \tag{4a}$$

$$\zeta=\frac{-i}{k^{[0]}L}(\ln(X\pm i\sqrt{1-X^2}))+\frac{2m\pi}{k^{[0]}L}, \tag{4b}$$

wherein $X=(1-S_{11}^2+S_{21}^2)/2S_{21}$ and m is an integer.

For a rigid frame porous plate, the signs in Eqs. (4a) and (4b) can be determined by the requirements $\mathrm{Re}(z)\geq0$ and

$\mathrm{Im}(z) \geq 0$ for Eq. (4a), and $\mathrm{Im}(\zeta) \geq 0$ for Eq. (4b). Both requirements result from the outgoing wave condition together with the Fourier transform convention. In fact, z and ζ are related and their relationship can be used to determine the sign in Eqs. (4a) and (4b) as reported in Ref. 24. Effectively, a small perturbation of S_{11} and S_{21} easily produced in experimental measurements may change the sign of $\mathrm{Re}(z)$ and $\mathrm{Im}(\zeta)$, making it impossible to satisfy the previous requirements, as discussed in Ref. 27. The derived method is particularly adapted when $\mathrm{Re}(z)$ and $\mathrm{Im}(\zeta)$ are close to zero and is also of impractical interest for rigid frame porous materials because $\mathrm{Re}(z)$ is always greater than unity. Nevertheless, once the value of z is obtained, ζ can be determined without sign ambiguity through

$$\zeta = \frac{-i}{k^{[0]}L}\left(\ln\left(\frac{S_{21}(z+1)}{z+1-S_{11}(z-1)}\right)\right) + \frac{2m\pi}{k^{[0]}L}. \tag{5}$$

The integer m related to the branch index of $\mathrm{Re}(\zeta)$ can be determined by the requirement $\mathrm{Re}(\zeta) \geq \sqrt{\alpha_\infty}$ [because $\mathrm{Re}(c^{[1]}(\omega)) \leq c^{[0]}/\sqrt{\alpha_\infty}$]. Its determination is not straightforward, because the requirement depends on one of the parameters to reconstruct.

The condition $\mathrm{Re}(\zeta) \geq 1$ should normally be sufficient for its correct determination, but problems occur for large α_∞ and/or for high frequency solicitation because of large $k^{[0]}L$. This usually leads authors to use small thickness sample. This problem can be solved by use of an iterative scheme. The latter is initialized with m as determined through the condition $\mathrm{Re}(\zeta) \geq 1$ and consists in adding 1 to the previously calculated m as long as the slope of $\mathrm{Re}(\zeta(\omega))$ is not negative. This condition is a mathematical translation of the fact that the phase velocity $c^{[1]}(\omega)$ associated with a rigid frame porous material is an increasing function of the frequency toward its high frequency limit $c^{[0]}/\sqrt{\alpha_\infty}$; i.e., $\mathrm{Re}(\zeta) = \mathrm{Re}(c^{[0]}/c^{[1]}(\omega))$ is a decreasing function of ω. The latter iterative scheme is chosen because the condition $\mathrm{Re}(\zeta) \geq 1$ can lead to an underevaluated m for large $k^{[0]}L$ and so an underevaluated ζ. The reconstructed value of α_∞ is then underevaluated and can reach a nonphysical value less than unity. An iterative scheme based on the reconstructed value of α_∞ is also of impractical interest.

Another condition for the correct determination of the integer m is connected to the fact that both effective density and bulk modulus should be continuous functions of frequency. This problem was not encountered during the experiments presented here, but is also related to large values of $k^{[0]}L$. The reader can also refer to Ref. 24, keeping in mind that the high frequency limit clearly defines the initialization of the continuity condition that must be applied.

B. Reconstruction of ϕ, α_∞, Λ, and Λ' from the high frequency approximation of the JCAM

Let us assume in what follows that z and ζ can be evaluated for frequencies ν ($\omega = 2\pi\nu$) in the interval $[\nu_1, \nu_2]$ over which the high frequency approximation of the JCAM is valid. The equivalent density and bulk modulus ratios reduce to

$$\tilde{\rho} = \frac{\rho^{[1]}}{\rho^{[0]}} = \frac{\alpha_\infty}{\phi}\left(1 + \frac{2}{\Lambda}\sqrt{\frac{i\eta}{\omega\rho_f}}\right),$$

$$\tilde{K} = \frac{K^{[1]}}{K^{[0]}} = \frac{1}{\phi}\left(1 + \frac{2(1-\gamma)}{\Lambda'}\sqrt{\frac{i\eta}{\omega\ \mathrm{Pr}\ \rho_f}}\right), \tag{6}$$

wherein $\mathrm{Pr} = 0.71$ is the Prandtl number.

Noting that $\tilde{K}(\omega) = z/\zeta$ and $\tilde{\rho}(\omega) = z\zeta$, several reconstruction algorithms can be developed for the recovery of the four parameters appealing to the high frequency approximation of the JCAM. The algorithm that was found to give the most accurate results is based on a phase and amplitude analysis of both the equivalent density and bulk modulus. At each frequency, a value $\bar{x}(\omega)$ of the parameter x is recovered analytically, $x = \phi$, α_∞, Λ, or Λ'. The final value of x is taken to be the average value of $\bar{x}(\omega)$ over $[\omega_1, \omega_2]$; i.e., $x = \mathrm{mean}[\bar{x}(\omega)]$. The latter operation regularizes the inverse problem.

From $\mathrm{Im}(\tilde{K})/\mathrm{Re}(\tilde{K})$ and $\mathrm{Im}(\tilde{\rho})/\mathrm{Re}(\tilde{\rho})$, which are both independent of α_∞ and ϕ, the two characteristic lengths are first recovered from

$$\bar{\Lambda} = \sqrt{\frac{2\eta}{\omega\rho_f}}\left(\frac{\mathrm{Re}(\tilde{\rho}) - \mathrm{Im}(\tilde{\rho})}{\mathrm{Im}(\tilde{\rho})}\right),$$

$$\bar{\Lambda}' = (1-\gamma)\sqrt{\frac{2\eta}{\omega\ \mathrm{Pr}\ \rho_f}}\left(\frac{\mathrm{Re}(\tilde{K}) - \mathrm{Im}(\tilde{K})}{\mathrm{Im}(\tilde{K})}\right). \tag{7}$$

Then, ϕ is recovered from $\|\tilde{K}\|$ via

$$\bar{\phi} = \frac{1}{\|\tilde{K}\|}\left(1 + \frac{2(1-\gamma)}{\Lambda'}\sqrt{\frac{2\eta}{\omega\ \mathrm{Pr}\ \rho_f}} + \frac{4(1-\gamma)^2\eta}{\Lambda'^2\omega\ \mathrm{Pr}\ \rho_f}\right)^{1/2}, \tag{8}$$

and finally α_∞ is recovered from $\|\tilde{\rho}\|$ by means of

$$\overline{\alpha_\infty} = \phi\|\tilde{\rho}\|\left(1 + \frac{2}{\Lambda}\sqrt{\frac{2\eta}{\omega\rho_f}} + \frac{4\eta}{\Lambda^2\omega\rho_f}\right)^{-1/2}. \tag{9}$$

III. EXAMPLE OF A RECONSTRUCTION FROM EXPERIMENTAL DATA

The method has been applied to efficiently characterize several homogeneous rigid frame porous samples (polyurethane foam, melamine foam, etc.) with low and medium flow resistivities.

In what follows, a $L = 27.5$ mm thick medium resistivity rigid frame porous material sample is considered. This material has already been characterized at various frequencies (100 and 200 kHz) in the ultrasonic range by some of the authors of the present paper,[18] wherein a smaller sample of 7 mm thick was employed. Its characteristic parameters were also previously determined by use of different methods[15,16] and are recalled in Table I. Its flow resistivity is $\sigma = 38\,000$ N m s^{-4} (measured with a flowmeter).

A. Experimental setup and procedure

The experimental setup is shown in Fig. 1. Two air-coupled piezoelectric Ultran NCG100-D25 transducers de-

TABLE I. Properties of the studied homogeneous material as recovered in Refs. 15 and 16, as recovered in Ref. 18, and as recovered with our analytic method.

	ϕ	α_∞	Λ (μm)	Λ' (μm)
Use of Refs. 15 and 16	0.7 ± 0.05	1.25 ± 0.05	50 ± 10	$3\times\Lambda=150\pm30$
Ref. 18	0.72–0.74	1.21–1.26	42–66	$3\times\Lambda=126$–198
Present method	0.752	1.246	55.4	178.4

noted Ta and Tb, whose central frequencies are 100 kHz, are placed at x_a and x_b. The airborne wave is generated by Ta and detected by Ta in the pulse-echo mode in the reflection experiments or by Tb in the transmission experiments. All recorded signals are averaged over 512 waveforms.

The method is very sensitive to small variations of the sample alignment during the recording of the reflected $p^r(x_a,t)$ and the transmitted $p^t(x_b,t)$ fields. The sample remains in place for the measurement of both of these fields, its first interface being placed at the origin of the Cartesian coordinate system such that $p^r(x_a,t)$ and $p^t(x_b,t)$ can be recorded over the same time window of the oscilloscope; i.e., the first interface of the sample is placed approximately at equal distance from the two transducers; i.e., $x_a \approx |x_b|$. This procedure avoids problems caused by temporal shift between the windows used to measure reflected or transmitted waves with and without the sample, which is a source of error as discussed in Ref. 28 for the reconstruction of ζ and z.

The main difficulty with ultrasonic measurements is the evaluation from the time domain responses of the frequency domain reflection and transmission coefficients $\mathcal{R}$ and $\mathcal{T}$, with sufficient accuracy for the inversion to be carried out, and over a sufficiently large interval of frequency for the inverse problem to be regularized. This operation requires particular care, because it is often considered to be highly uncertain and/or ill-posed. This has led some authors to prefer a time domain inversion algorithm based on fractional derivatives[17,18] or to use time domain deconvolution.

The Fourier transforms of $p^r(x_a,t)$ and $p^t(x_b,t)$ are related to $\mathcal{R}$ and $\mathcal{T}$ through

$$P^r(x_a) = \mathcal{R}A^i e^{ik^{[0]}x_a} = \mathcal{T}P^{ri}(x_a),$$

$$P^t(x_b) = \mathcal{T}A^i e^{-ik^{[0]}x_b} = \mathcal{T}P^i(x_b), \tag{10}$$

wherein $A^i(\omega)$ is the spectrum of the incident field, $P^i(x_b)$ is the incident field as recorded with T_b in absence of the sample, and $P^{ri}(x_a)$ corresponds to time delay of the reflected field between the first interface of the sample and the location of T_a. The latter field, abusively called here "incident field," can be recorded in time domain with T_a in pulse-echo mode when a perfectly reflecting plate is placed such that its first interface is located at the origin. Any time delay between $p^{ri}(x_a,t)$ and $p^r(x_a,t)$ is expected if the first interface of the sample and the perfectly reflecting plate are located at the same position. Nevertheless, to avoid such source of error, $p^r(x_a,t)$ is translated in time in such a way that its maximum of amplitude occurs at the same time as the one of $p^{ri}(x_a,t)$. The frequency domain reflection and transmission coefficients are then evaluated by means of $\mathcal{R}=P^r(x_a,\omega)/P^{ri}(x_a,\omega)$ and $\mathcal{T}=P^t(x_b,\omega)/P^i(x_b,\omega)$ over the intersection of the two −3 dB bandwidths as calculated for $P^{ri}(x_a,\omega)$ and $P^i(x_b,\omega)$. These bandwidths are effectively different because the latter incorporate, to some extent, transfer functions of the transducers T_a and T_b, which are close but not identical.

In addition, the amplitude of $p^r(x_a,t)$ is often very small with a very poor signal to noise ratio (SNR) for relatively low and medium flow resistivity porous materials. The noise in a signal is usually assumed to be a stationary random process; i.e., its mean value is independent of the time origin. In the experiments, the acquisitions are done using a triggering process, which ensures the time origin of the signals. Recorded signals are averaged. The averaging operation induces a large decrease in the noise that is incoherent with respect to the trigger signal. Therefore, the main part of the remaining noise is coherent[29] with the trigger signal, which is the same for all the experiments. The remaining noise is mainly electronic from the measurement devices. In the reflection experiments only one transducer is used. To get rid of this remaining noise component, which is coherent, reproducible, and somewhat synchronized with the trigger, the latter, called $p^n(x_a,t)$, is recorded without the sample and perfectly reflecting plate, the emission being still on (the experimental setup is identical). The incident and reflected fields used for the inversion are $\widetilde{p^r}(x_a,t)=p^r(x_a,t)-p^n(x_a,t)$ and $\widetilde{p^{ri}}(x_a,t)=p^{ri}(x_a,t)-p^n(x_a,t)$, as shown Fig. 2 for $\widetilde{p^r}(x_a,t)$.

For highly absorbent foam and/or large flow resistivity porous material, a similar procedure can be employed to determine $\widetilde{p^t}(x_b,t)$ and $\widetilde{p^i}(x_b,t)$, by a prior recording of $p^n(x_b,t)$ with T_b, without the sample and by turning off the excitation delivered by T_a. This procedure is certainly less efficient than the one described for the experiment in reflection because two transducers are needed in transmission experiments, this imposing the excitation to be switched off.

In summary, the incident fields are recorded, without the sample, as follows: (1) Record $p^i(x_b,t)$ using Tb, (2) record the noise $p^n(x_a,t)$ using Ta in pulse-echo mode, (3) place an infinitely rigid plate (here an aluminum plate is used) whose first interface is located at the origin, and (4) record $p^{ri}(x_a,t)$

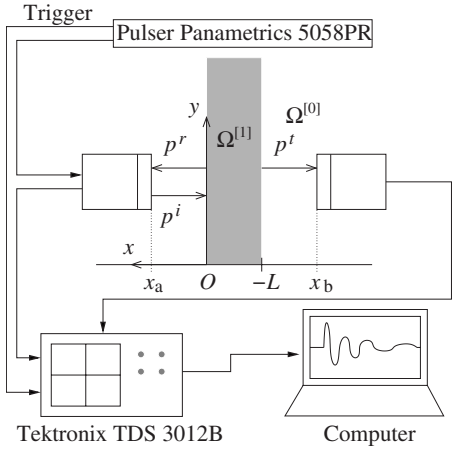

FIG. 1. Experimental setup and description of the configuration. The transducers are Ultran NCG100-D25 air-coupled piezoelectric transducers.

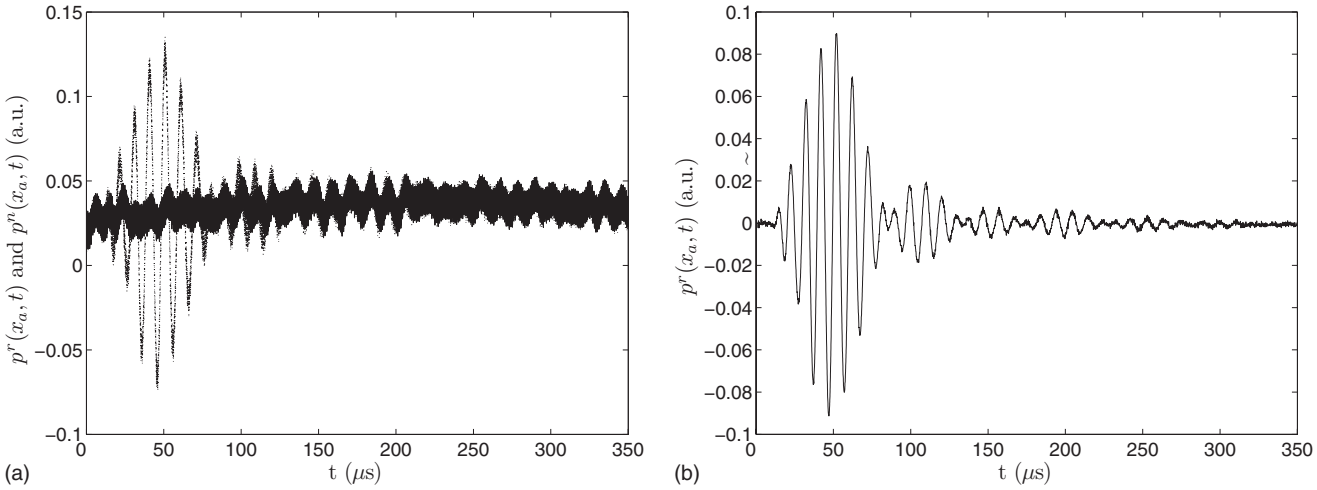

FIG. 2. (a) $p^r(x_a,t)$ (dotted curve) and $p^n(x_a,t)$ (solid curve) as recorded on the oscilloscope and (b) $\widetilde{p^r}(x_a,t)$ as used for the inversion.

using Ta in pulse-echo mode. The infinitely rigid plate is then replaced with the sample, carefully placed at the origin, and $p^r(x_a,t)$ is recorded in the pulse-echo mode using Ta while $p^t(x_b,t)$ is recorded employing Tb.

B. Numerical reconstruction from experimental data

Once m is correctly determined, the following parameters are recovered from $\bar{\phi}(\nu)$, $\overline{\alpha_\infty}(\nu)$, $\bar{\Lambda}(\nu)$, and $\overline{\Lambda'}(\nu)$,

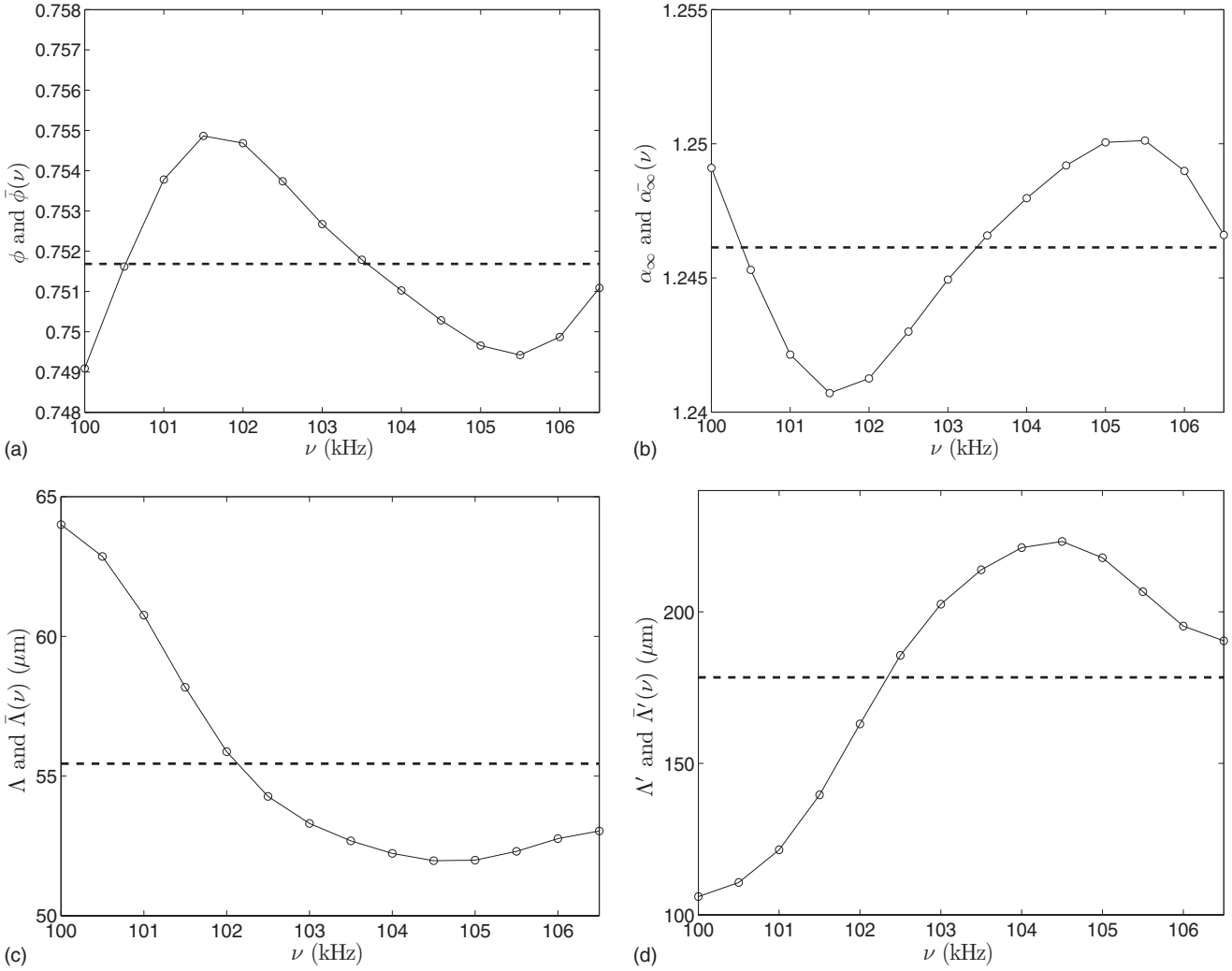

FIG. 3. (a) $\bar{\phi}(\nu)$ (solid curve) and its average value ϕ (dashed line), (b) $\bar{\alpha}_\infty(\nu)$ (solid curve) and its average value α_∞ (dashed line), (c) $\bar{\Lambda}(\nu)$ (solid curve) and its average value Λ (dashed line), and (d) $\overline{\Lambda'}(\nu)$ (solid curve) and its average value Λ' (dashed line). The frequency range corresponds to the intersection of the two −3 dB bandwidths as calculated for $\widetilde{P^{ri}}(x_a,\omega)$ and $P^i(x_b,\omega)$.

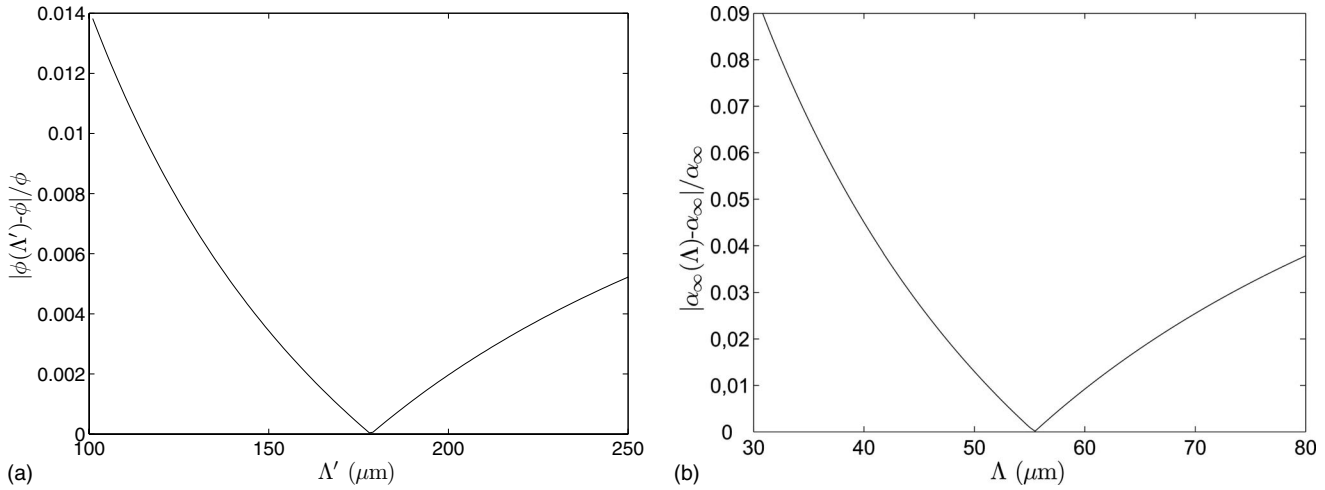

FIG. 4. Absolute value of the relative error of the recovered parameter ϕ as a function of Λ' (a) and α_∞ as a function of Λ (b), over the frequency bandwidth used for the reconstruction.

which are plotted in Fig. 3: $\phi=0.752$, $\alpha_\infty=1.246$, $\Lambda=55.4$ μm, and $\Lambda'=178.4$ μm. These parameters agree with those found in Ref. 18 via a time domain method and other ultrasonic methods[15,16] (see Table I). The unbiased estimators of the standard deviation, as calculated for the vector x as $s(x)=\sqrt{1/(n-1)\Sigma_{i=1}^{n}(x_i-\text{mean}(x))^2}$, are $s(\phi)=2\times10^{-3}$, $s(\alpha_\infty)=3.3\times10^{-3}$, $s(\Lambda)=4.25$ μm, and $s(\Lambda')=42.3$ μm. The latter estimator for Λ' seems large at first glance, but the constraint $\Lambda'=3\Lambda$ used in Ref. 18 leads to a value $\Lambda'=150\pm30$ μm, whose error is also of the same order as $s(\Lambda')$. The latter constraint, i.e., $\Lambda'=3\Lambda$, is debatable because the value of Λ' is usually between 2Λ and 3Λ for most of the porous foams.[22]

A specific feature of the reconstruction of the parameters appealing to the high frequency approximation of the JCAM is the fact that for given S_{11} and S_{21}, the reconstruction of ϕ through Eq. (8) is, as expected, rather insensitive to a variation of Λ', Fig. 4. Likewise, the influence of $s(\Lambda')$ is not significant on the reconstruction of the other parameters. The reconstruction of α_∞ is strongly sensitive on Λ, Fig. 4.

The reconstructed normalized density and bulk modulus, as calculated by introducing the reconstructed parameters in Eq. (6), over the frequency range used for the reconstruction are in good agreement with the measured ones, Fig. 5. It is clear that the developed analytic method for the recovery of the characteristic parameters realizes some kind of least squares fitting of both density and bulk modulus. This fit is much more efficient than a direct fitting of the curve. For example, use of an algorithm based on a basic fit of $\text{Im}(\rho^{[1]}/\rho^{[0]})$, which is theoretically equal to $1/\Lambda\sqrt{2\eta/\omega\rho_f}$, leads to a negative value of Λ because the experimental slope is clearly positive. Use of such an algorithm would require reconstructions over a larger frequency range.

The time domain reconstructed reflected and transmitted fields, as calculated from the reconstructed parameters introduced in Eqs. (6) and (2) via inverse Fourier transform of Eq. (10), $P^{ri}(x_a)$ and $P^{i}(x_b)$ being the measured incident signals, agree quite well with the experimentally recorded fields, Fig. 6. The Bravais–Pearson linear correlation coefficients between the latter fields are 0.9811 in reflection and 0.9819 in transmission.

The method was applied to characterize various samples with other piezoelectric Ultran transducers, whose central frequency is 200 kHz. Table II presents the values of the parameters as recovered with the present method and as recovered with other ultrasonic methods.[15–17] The flow

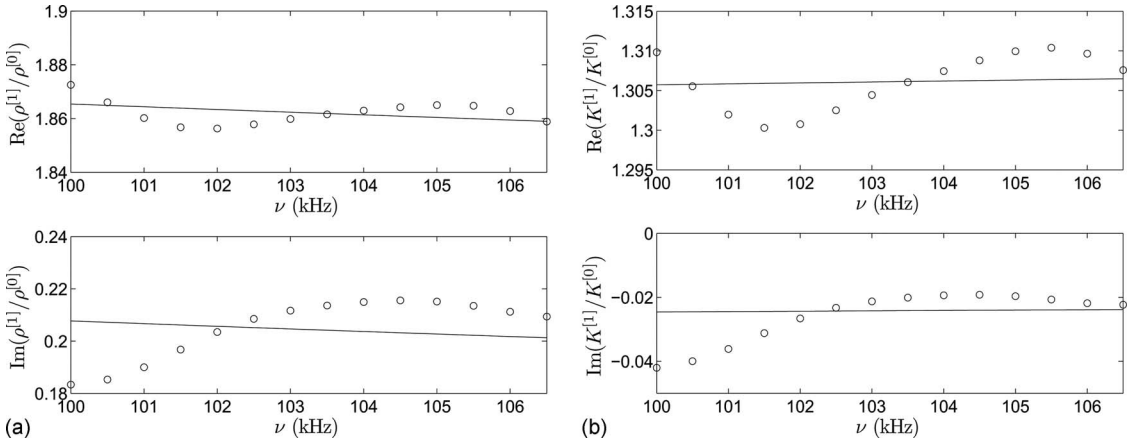

FIG. 5. Comparison between experimental (o) and reconstructed (—) real and imaginary parts of (a) the normalized density $\tilde{\rho}$ and (b) the bulk modulus $\tilde{K}$.

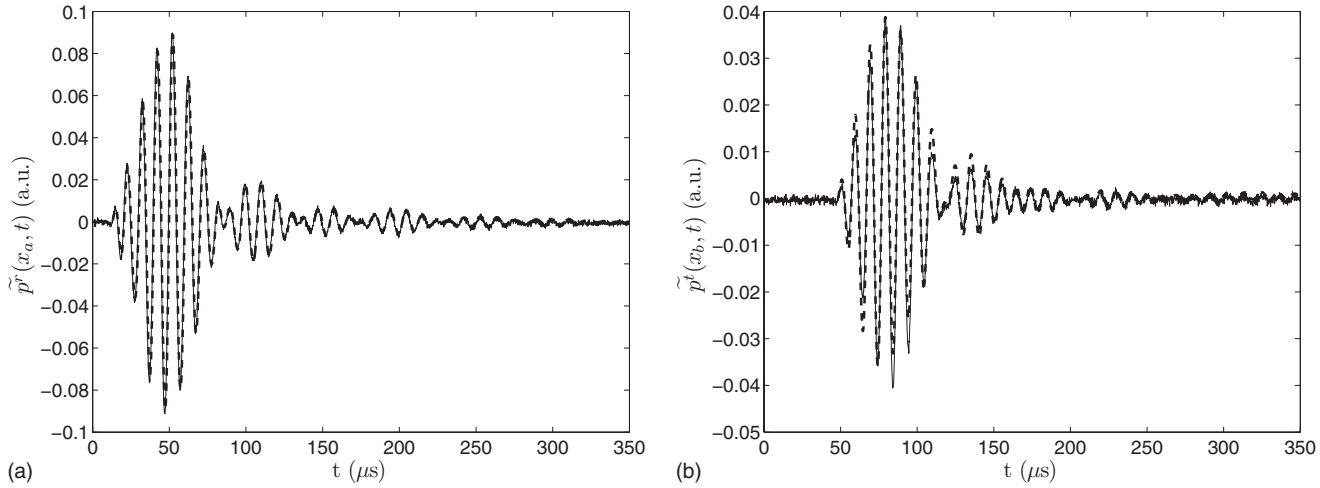

FIG. 6. Comparison between experimental (—) and simulated (– – –) signals, with recovered $\phi=0.752$, $\alpha_\infty=1.246$, $\Lambda=55.4$ μm, and $\Lambda'=178.4$ μm: (a) reflected signal and (b) transmitted signal.

resistivity of the polyurethane foam is low, i.e., $\sigma=2830$ N m s^{-4}, while the one of the melamine is $\sigma=12\,000$ N m s^{-4}.

C. Discussion

The method is sensitive to the approximation of the continuous Fourier transform by a discrete one and to the temporal shift, especially for the evaluation of S_{11}, as was pointed out in Ref. 28. Nevertheless, assuming that the Fourier transformed is correctly performed, and that the proposed process does not lead to temporal shift, other sources of error arise.

From

$$\frac{\partial z^2}{\partial S_{21}}=\frac{8S_{21}S_{11}}{((1-S_{11})^2-S_{21}^2)^2},$$

$$\frac{\partial z^2}{\partial S_{11}}=\frac{4(1-S_{11}^2-S_{21}^2)}{((1-S_{11})^2-S_{21}^2)^2}, \tag{11}$$

it is obvious that a weak transmission, i.e., large flow resistivity materials, has little influence on the retrieval of z. For the low and medium flow resistivity foams tested, S_{11} is close to zero. The reconstruction is also highly sensitive when S_{21} is close to one, which is in contradiction with the use of thin layer sample, for which reconstruction is much more efficient. On the other hand, from

$$\frac{\partial \zeta}{\partial S_{11}}=\frac{-1}{ik^{[0]}L}\frac{z-1}{z+1-S_{11}(z-1)},$$

$$\frac{\partial \zeta}{\partial S_{21}}=\frac{-1}{S_{21}ik^{[0]}L}, \tag{12}$$

it is obvious that ζ, for S_{11} close to zero, is rather insensitive to S_{11}, while it is very sensitive to S_{21} when the latter is close to zero. This also imposes conditions not only on the absorption of the sample to characterize, but also on its thickness: both should be small. This method seems particularly adapted to low and medium resistive materials, but less to highly resistive ones, for which S_{21} vanishes.

On the other hand, it is obvious from Eq. (7) that Λ and Λ' are, respectively, highly sensitive to $\mathrm{Im}(\tilde{\rho})$ and $\mathrm{Im}(\tilde{K})$, when the latter is small. Particularly, the reconstructed characteristic lengths are singular when the imaginary part of the density or of the bulk modulus vanishes. Both of these quantities are close to zero in the asymptotic high frequency regime of the JCAM. The regularization process partly avoids such problems, but decreasing the frequency of the solicitation is the best way to increase the value of both imaginary parts. From Eqs. (8) and (9), it is clear that reconstructed porosity is highly sensitive to $\|\tilde{K}\|$ when the latter is small, while the reconstructed tortuosity is less sensitive to variation of $\|\tilde{\rho}\|$.

One of the biggest limitations of the present method is closely linked to experiments, and particularly to the SNR for the evaluation of the reflection coefficient. The flow resistivity of the sample should not be very small. Effectively, very low resistivity foams exhibit quasi-null reflected fields. Their characterization by the present method is also impossible. A similar remark arises for highly resistive porous material, such as rock wool, which exhibits quasi-null transmitted fields.

TABLE II. Properties of other homogeneous materials as recovered with Refs. 15–17 and as recovered by our analytic method.

	L (mm)	ϕ	α_∞	Λ (μm)	Λ' (μm)
Melamine foam					
Use of Refs. 15–17	10	0.99	1.001	150	250
Present method		0.99	1.011	159.2	259.2
Polyurethane foam					
Use of Refs. 15–17	27	0.97	1.07	270	670
Present method		0.975	1.057	319.4	621

Another limitation is strongly linked to ultrasonic measurements, for which $k^{[0]}L$ is high. This induces possible difficulties in the evaluation of the correct branch of $\mathrm{Re}(\zeta)$. The frequency band used to perform the inversion, chosen to be the intersection of the -3 dB bandwidth of both Fourier transform of the recorded fields by T_a and T_b without sample, is thin. Use of larger band transducers should help in the regularization of the inverse problem and in its resolution. In this case, particular care should be paid to the frequency range used for the reconstruction, in a sense the model should be valid. Check of the constancy and to some extent to the continuity of the recovered parameters over the frequency range, as proposed in Refs. 9 and 10, should avoid this possible problem.

One of the main advantages of the present method is that the reconstructed parameters are not constrained, as it is usually the case when minimization techniques are applied. On the other hand, this is also a disadvantage because nonphysical values, such as negative characteristic lengths, porosity larger than 1, or tortuosity smaller than 1, can be reconstructed if experiments are not performed with sufficient care. Moreover, among all the experiments performed, it was found that whatever the reconstructed parameters are, even nonphysical ones, the reconstructed time domain signals are always in agreement with the experimental ones. An a priori correct ratio between the reconstructed Λ' and Λ seems to be indicative of the quality of the experiments, and leads to the accurate reconstructions of the other parameters. This a priori is connected to the type of material tested. For most of the industrial foams, a ratio Λ'/Λ that lies between 2 and 3 seems to be a good indicator of the reconstruction. For other industrial porous materials, other ratios can be used, for example, a ratio close to 2 for fibrous materials.

It is then important to check the consistency of the recovered parameters with regard to the frequency of solicitation in order to validate the use of the asymptotic high frequency JCAM. This can be simply achieved at high frequency (diffusion limit) by checking if the wavelength of the central frequency of the incident field is larger than the thermal characteristic length. Effectively, the latter characteristic length represents a measure of the average pore size (although the "pore" is not always straightforwardly defined) while the viscous characteristic length corresponds to the average size of the "constrictions" in the porous medium,[22] i.e., the average distance between pore walls in the narrower areas of the pore volume. For example, the ratio of the wavelength in air at 100 kHz over the recovered value of Λ' for the first medium resistivity porous sample studied in this article is around 19. As stated in the Introduction, the low frequency bound of the asymptotic high frequency JCAM being not clear, it is then quite difficult to validate the use of the dissipation model with regard to the latter, particularly because the flow resistivity is not recovered through our method and despite the fact that a frequency higher than 100 kHz usually ensures this validation. Nevertheless, this problem can be partly solved by performing ultrasonic experiments for various central frequencies of the transducers, for example, at 100 and 200 kHz, keeping in mind that the dissipation model should be valid, that additional problems related to large $k^{[0]}L$ could occur, and that a correct SNR is required. If the reconstructed parameters are quite similar, the constancy of the dissipation model and so of the reconstructed parameters is achieved. This operation is similar to use of larger band transducers, in the sense it would help the regularization of the problem, when the dissipation model is valid.

IV. CONCLUSION

A frequency domain method has been developed, which allows the analytic reconstruction of the four parameters appealing to the high frequency approximation of the JCAM (porosity, tortuosity, and thermal and viscous characteristic lengths) for macroscopically homogeneous rigid frame porous materials. The reconstruction is achieved by first retrieving the complex and frequency-dependent acoustic index of refraction and impedance ratio, from which the four latter parameters are reconstructed. The method and algorithm were tested on relatively low and medium flow resistivity porous samples, which mainly cover the range of resistivity values of plastic foams, and its accuracy has been demonstrated in the ultrasonic domain on three materials. The experiments must be very precise even if the reconstructed time traces are very close to the experimental ones. This is to avoid reconstructed parameters that are meaningless. This situation is often avoided when minimization techniques are used to solve inverse problems. It was found empirically that when the ratio of the recovered thermal and viscous characteristic lengths lies between 2 and 3, as it is the case for most industrial foams, the experiments are performed with sufficient efficiency and the recovered parameters turn out to be accurate.

For the reconstruction to be performed, time domain reflected and transmitted signals should be recorded with a high SNR. Some methods have been employed here to increase the SNR, especially for the reflected field, but it also imposes some constraints on the materials that can be tested with the present method. The flow resistivity should not be very small for the record of the reflected field, while it should not be very large for the record of the transmitted field.

This algorithm being based on analytic developments, further investigations should lead to the development of a more complex algorithm for the complete analytic characterization of homogeneous foam samples, i.e., the recovery of additional parameters such as the flow resistivity from additional lower frequency measurements or parameters of other models relevant for mid frequency range, for example. This method can be viewed as a complementary to the low frequency method developed in Refs. 9 and 10 in the sense that it allows the recovery of the porosity, which should be known in Refs. 9 and 10. The other recovered parameters in the two frequency ranges may then be compared.

ACKNOWLEDGMENT

The authors would like to thank A. Wirgin for his useful help during the experiments and the writing of this paper.

[1]M. Biot, "Theory of propagation of elastic waves in a fluid-saturated porous solid—I. Low frequency range," J. Acoust. Soc. Am. **28**, 168–178 (1956); M. Biot, "Theory of propagation of elastic waves in a fluid-saturated porous solid—II. High frequency range," J. Acoust. Soc. Am. **28**, 179–191 (1956).
[2]M. Biot, "Mechanics of deformation and acoustic propagation in porous media," J. Appl. Phys. **33**, 1482–1498 (1962).
[3]D. Johnson, J. Koplik, and R. Dashen, "Theory of dynamic permeability and tortuosity in fluid-saturated porous media," J. Fluid Mech. **176**, 379–402 (1987).
[4]Y. Champoux and J. Allard, "Dynamic tortuosity and bulk modulus in air-saturated porous media," J. Appl. Phys. **70**, 1975–1979 (1991).
[5]K. Attenborough, "Acoustical characteristics of porous materials," Phys. Rep. **82**, 179–227 (1982).
[6]D. Lafarge, P. Lemarinier, J.-F. Allard, and V. Tarnow, "Dynamic compressibility of air porous structures at audible frequencies," J. Acoust. Soc. Am. **102**, 1995–2006 (1997).
[7]D. Wilson, "Relaxation-matched modeling of propagation through porous media, including fractal pore structure," J. Acoust. Soc. Am. **94**, 1136–1145 (1993).
[8]L. De Ryck, J.-P. Groby, P. Leclaire, W. Lauriks, A. Wirgin, Z. Fellah, and C. Depollier, "Acoustic wave propagation in a macroscopically inhomogeneous porous medium saturated by a fluid," Appl. Phys. Lett. **90**, 181901 (2007).
[9]R. Panneton and X. Olny, "Acoustic determination of the parameters governing viscous dissipation in porous media," J. Acoust. Soc. Am. **119**, 2027–2040 (2006).
[10]X. Olny and R. Panneton, "Acoustic determination of the parameters governing thermal dissipation in porous media," J. Acoust. Soc. Am. **123**, 814–824 (2008).
[11]L. L. Beranek, "Acoustic impedance of porous materials," J. Acoust. Soc. Am. **13**, 248–260 (1942).
[12]R. Brown and R. Bolt, "The measurement of flow resistance of porous acoustic materials," J. Acoust. Soc. Am. **13**, 337–344 (1942).
[13]Y. Champoux, M. Stinson, and G. Daighle, "Air-based system for the measurement of porosity," J. Acoust. Soc. Am. **89**, 910–916 (1991).
[14]J. Allard, B. Castagnede, M. Henry, and W. Lauriks, "Evaluation of tortuosity in acoustic porous materials saturated by air," C. R. Acad. Sci. **322**, 754–755 (1994).
[15]Z. Fellah, S. Berger, W. Lauriks, C. Depollier, C. Aristégui, and J.-Y. Chapelon, "Measuring the porosity and the tortuosity of porous materials via reflected waves at oblique incidence," J. Acoust. Soc. Am. **113**, 2424–2433 (2003).
[16]P. Leclaire, L. Kelders, W. Lauriks, N. Brown, M. Melon, and B. Castagnède, "Determination of the viscous and thermal characteristic lengths of plastic foams by ultrasonic measurements in helium and air," J. Appl. Phys. **80**, 2009–2012 (1996).
[17]Z. Fellah, C. Depollier, S. Berger, W. Lauriks, P. Trompette, and J.-Y. Chapelon, "Determination of transport parameters in air-saturated porous materials via reflected ultrasonic waves," J. Acoust. Soc. Am. **114**, 2561–2569 (2003).
[18]Z. Fellah, F. Mitri, M. Fellah, E. Ogam, and C. Depollier, "Ultrasonic characterization of porous materials: Inverse problem," J. Sound Vib. **302**, 746–759 (2007).
[19]C. Ayrault and S. D. Griffiths, "Separation of viscothermal losses and scattering in ultrasonic characterization of porous media," Ultrasonics **45**, 40–49 (2006).
[20]L. De Ryck, W. Lauriks, P. Leclaire, J.-P. Groby, A. Wirgin, and C. Depollier, "Reconstruction of material properties profiles in one-dimensional macroscopically inhomogeneous rigid frame porous media in the frequency domain," J. Acoust. Soc. Am. **124**, 1591–1606 (2008).
[21]H. Utsuno, T. Tanaka, and T. Fujikawa, "Transfer function method for measuring characteristic impedance and propagation constant of porous materials," J. Acoust. Soc. Am. **86**, 637–643 (1989).
[22]J.-F. Allard, *Propagation of Sound in Porous Media: Modeling Sound Absorbing Materials* (Chapman and Hall, London, 1993).
[23]J.-P. Groby, L. De Ryck, P. Leclaire, A. Wirgin, W. Lauriks, R. P. Gilbert, and Y. S. Xu, "Use of specific Green's functions for solving direct problems involving a heterogeneous rigid frame porous medium slab solicited by acoustic waves," Math. Methods Appl. Sci. **30**, 91–122 (2007).
[24]X. Chen, T. Grzegorczyk, B. Wu, J. Pacheco, and J. Kong, "Robust method to retrieve the constitutive effective parameters of metamaterials," Phys. Rev. E **70**, 016608 (2004).
[25]P. Markos and C. Soukoulis, "Transmission properties and effective electromagnetic parameters of double negative metamaterials," Opt. Express **11**, 649–661 (2003).
[26]R. Smith, S. Schultz, P. Markos, and C. Soukoulis, "Determination of effective permittivity and permeability of metamaterials from reflection and transmission coefficients," Phys. Rev. B **65**, 195104 (2002).
[27]R. Ziolkowski, "Design, fabrication, and testing of double negative metamaterials," IEEE Trans. Antennas Propag. **51**, 1516–1529 (2003).
[28]A. Nicolson, "Measurement of the intrinsic properties of materials by time domain techniques," IEEE Trans. Instrum. Meas. **19**, 377–382 (1970).
[29]J. S. Bendat and A. G. Piersol, *Engineering Application of Correlation and Spectral Analysis* (Wiley, New York, 1993).